STUDIA UBB CHEMIA, LXI, 3, Tom I, 2016 (p. 239-249)
(RECOMMENDED CITATION)

Dedicated to Professor Luminița Silaghi-Dumitrescu on the occasion of her 65th anniversary

INFLUENCE OF MgO/SiO_2 RATIO AND ADDITIVES ON BIONANOFORSTERITE POWDERS CHARACTERISTICS

LILIANA BIZO[a], MARIA GOREA[a,*], GABRIEL KATONA[a]

ABSTRACT. Forsterite (Mg_2SiO_4) powders were synthesized by solid state reaction from basic magnesium carbonate and silicon dioxide. The MgO/SiO_2 molar ratio was established at 2:1, 2:1.05 and 2:1.10. In order to realize a complete reaction between compounds and avoiding the MgO (periclase) presence in the final product, an excess of SiO_2 was added. Boric acid in small quantity was used as a mineralizer. The six mixtures were designed and prepared in the laboratory. After a good homogenization and mechanical activation, the raw mixtures were thermally treated at 800 °C, 900 °C, 1000 °C, 1200 °C, 1300 °C and 1350 °C with a heating rate of 2 °C/min and one hour plateau at maximum temperature. The grain size distribution of the powders obtained at 800 °C, 900 °C and 1000 °C, according to the particle analyzes, are in the nanometer range. Increasing the temperature the size of grains is increased at micrometer dimensions indicating the presence of agglomerates. The mineralogical compositions evidenced by X-ray powder diffraction (XRPD) showed as the main crystalline compound the forsterite beginning of 1200 °C temperature. The crystallinity index of forsterite depends on the thermal treatment conditions, being highest at 1350 °C. A small quantity of MgO at the maximum temperature in compositions without boric acid was identified. The shape and morphology of forsterite crystals were evidenced by TEM analyses.

Keywords: *nano forsterite, biomaterial, synthesis*

[a] *Babeş Bolyai University, Faculty of Chemistry and Chemical Engineering, 11 Arany Janos str., RO-400028, Cluj-Napoca, Romania,*
** Corresponding author: mgorea@chem.ubbcluj.ro*

INTRODUCTION

Due to the increasing interest in silicon and magnesium based bioceramic materials, much research was carried out recently on forsterite (Mg_2SiO_4) ceramics for medical applications [1-2]. Naghiu et al demonstrated that presence of MgO in small quantity does not affect the forsterite powder biocompatibility [3].

It was previously demonstrated that magnesium and silicon play an important role in human body processes: magnesium is one of the most important elements in the human body, closely associated with mineralization of calcined tissues and indirectly influences mineral metabolism, whereas silicon is an essential element in skeletal development. Recent research has shown that the compounds in the $MgO–SiO_2$ system are biocompatible, thus they are suitable to be used for dental and orthopaedic prosthetic materials.

Forsterite nanostructured ceramics show improved biocompatibility, superior mechanical properties and increased osteoblast adhesion and proliferation over normal materials [4]. Because nanoparticle ceramics show more attractive properties than microstructured ceramics, like high diffusion rates or mechanical properties, many methods have been employed for obtaining forsterite nanoparticles. These methods included sol–gel method [5-8], polymer precursor method [9], co-precipitation [10], or conventional solid-state reaction [11-16]. During the synthesis by the ceramic method, a reaction in solid phase, at high temperature between, MgO and SiO_2 takes place [17]. The formation of a single phase, forsterite, in the oxide systems $MgO-SiO_2$, is difficult to obtain. It is always accompanied by secondary phases like enstatite ($MgSiO_3$) and/or periclase (MgO). The mechanical activating of raw mixtures was demonstrated to be an efficient method to increase the chemical homogeneity of the product and to reduce the reaction temperature [18-20]. In this work boric acid as a mineralizing agent and a small excess of SiO_2 were used in order to enhance the nanostructure forsterite formation.

The aim of this work is to study the parameters of synthesis and characterization of nanoforsterite powders with a small excess of silicon dioxide. The effect of MgO/SiO_2 ratio and additives on bionanoforsterite powders characteristics will be investigated by different methods: X-ray powder diffraction (XRPD), particle size analysis and transmission electron microscopy (TEM).

RESULTS AND DISCUSSION

X-ray powder diffraction

X-ray powder diffraction (XRPD) patterns show the formation of well-crystallized forsterite in the samples thermally treated at 1350 °C. Beside of a forsterite phase, small quantities of periclase and enstatite were

detected in tested samples depending on composition and thermal treatment. The presence of the secondary phases could be assigned to an incomplete reaction or insufficient homogeneity of the precursor mixtures.

Figure 1 showed the XRPD pattern for samples DPI which is similar to DPII, composition without boric acid. It can observe that in the pattern of samples thermally treated at low temperatures (800 °C, 900 °C, 1000 °C) the presence of forsterite crystals is not evidenced. The only crystalline phase is periclase resulted from magnesium carbonate decomposition. In the samples treated at higher temperatures, 1200 °C, 1300 °C and 1350 °C, the specific peaks for forsterite as the main crystalline compound, and small quantities of enstatite and periclase were identified. In conclusion, in composition DPI and DPII, the reaction between reactants is no completed at 1350 °C temperature.

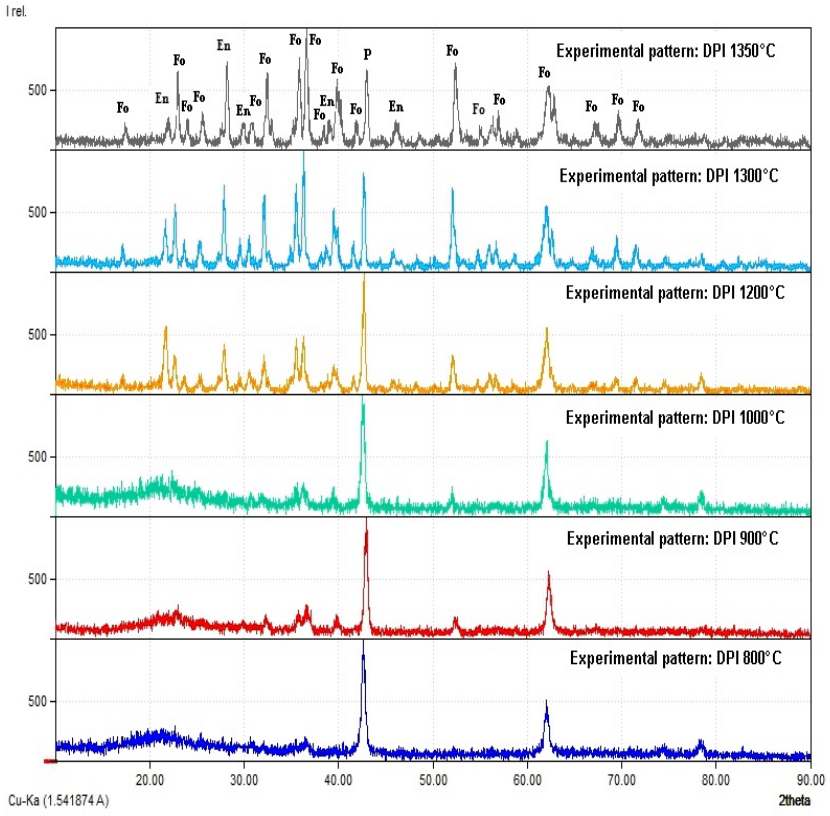

Figure 1. XRPD patterns of DPI samples treated at 800 °C, 900 °C, 1000 °C, 1200 °C, 1300 °C and 1350 °C, respectively (Fo-forsterite, En-enstatite, P-periclase)

In Figure 2 are presented the specific XRPD patterns of sample DPIII which are similar to DPIV at different temperatures.

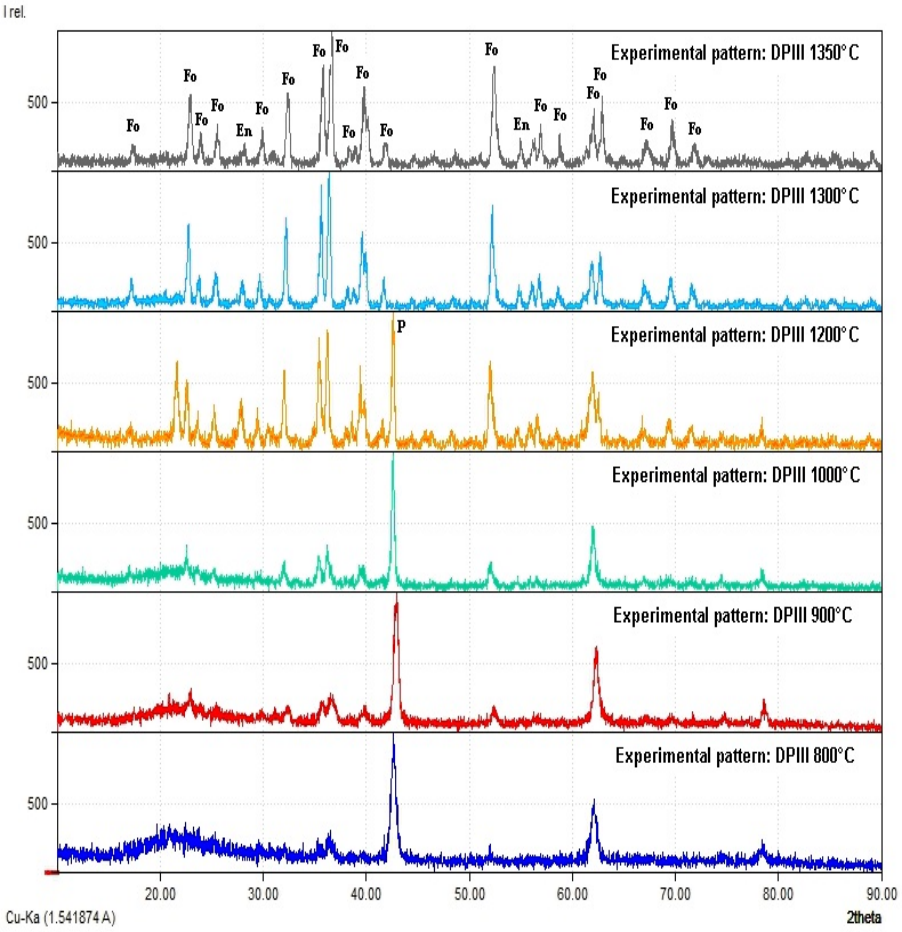

Figure 2. XRPD patterns of DPIII samples treated at 800 °C, 900 °C, 1000 °C, 1200 °C, 1300 °C and 1350 °C, respectively (Fo-forsterite, En-enstatite, P-periclase)

At low temperatures (800 °C, 900 °C, 1000 °C), the well crystalline phase evidenced is periclase and the enstatite and forsterite crystals are poorly crystalline. Beginning with 1200 °C temperature, the enstatite and forsterite phases were identified besides of periclase. At 1350 °C temperature the specific peaks of periclase and enstatite disappeared. This fact demonstrated that the presence of additives (boric acid) determines a complete reaction between reactants.

Figure 3 shows the XRPD specific pattern for samples DPV (similarly with DPVI) thermally treated at different temperatures.

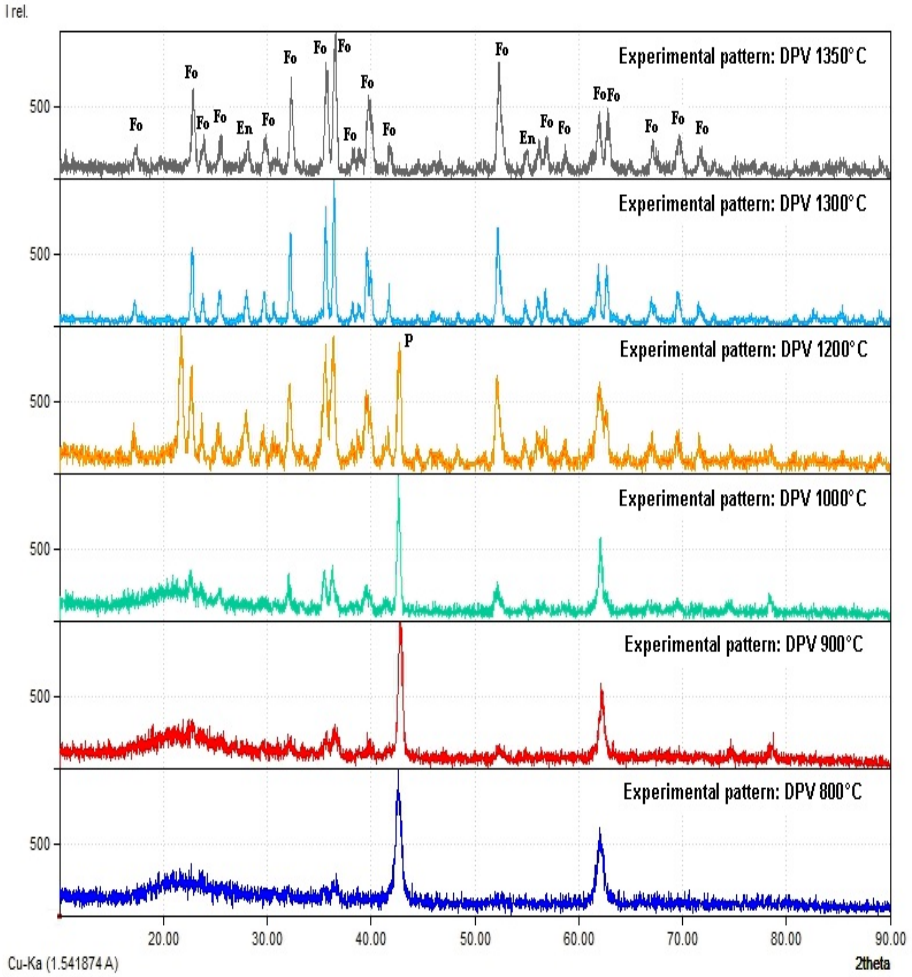

Figure 3. XRPD patterns of DPV samples treated at 800 °C, 900 °C, 1000 °C, 1200 °C, 1300 °C and 1350 °C, respectively (Fo-forsterite, En-enstatite, P-periclase)

The crystalline components evidenced by X-ray diffraction are similar to those detected in sample DPIII. At 1350 °C temperature only the forsterite and enstatite crystals were identified. It could be concluded that a small excess of SiO_2 and mainly a proper additive determine a complete reaction and obtaining of forsterite of nanometer size besides of small amounts of enstatite.

In table 1 are listed the crystallite values of forsterite calculated from XRPD data using Scherrer formula at 1200 °C, 1300 °C and 1350 °C, respectively temperatures.

Table 1. Calculated crystallite sizes D (nm)

Sample	D [nm]		
	1200 °C	1300 °C	1350 °C
DPI	21.90	25.43	23.87
DPII	29.21	24.63	21.30
DPIII	23.90	27.18	20.20
DPIV	26.28	26.28	21.30
DPV	14.08	29.20	19.70
DPVI	20.22	24.63	20.73

The calculated crystallite values for all the tested samples are in the 20 nm and 30 nm range size excepting the value of 14.08 nm for DPV sample.

Transmission Electron Microscopy – TEM

TEM microscopy evidenced the morphology and sizes of the crystallites from the synthesized powders (figure 4).

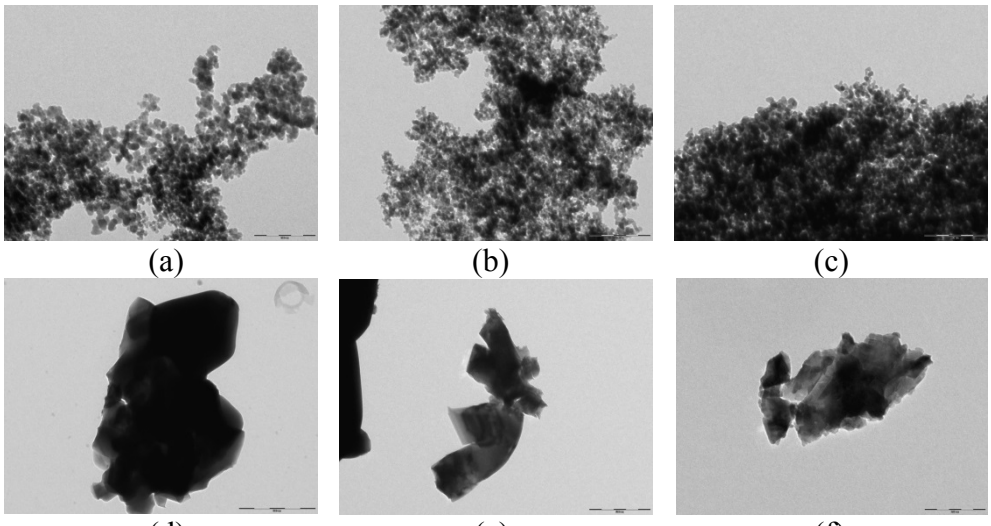

Figure 4.TEM images of forsterite powders at different temperatures:
(a) DPIV at 800 °C, (b) DPVI at 900 °C, (c) DPII at 1000 °C and (d) DPI at 1350 °C, (e) DPIII at 1350 °C, (f) DPV at 1350 °C

The TEM images show two types of crystal mixtures. In the samples fired at low temperatures very small and poorly crystalline phases are evidenced. The grain agglomerate and no individual crystal are illustrate (figure 4 a, b and c). In the case of samples fired at 1350 °C temperature the crystals orthoromboidal bipyramidal with a high crystallinity index specific for forsterite are identified. The crystal size are in the nanometer interval.

Grain size distribution

The grain size distribution of experimented composition thermally treated at 800 °C, 900 °C, 1000 °C is presented in figure 5.

The grain sizes of samples free of boric acid, DPI and DPII, are smaller than the others. This fact could be explained by agglomerates formation. The boric acid in the forsterite samples emphasizes the particles aggregation; due to agglomeration, there could not be stabilized a correlation between grain size and synthesis temperature.

The mean grain sizes of all treated samples with boric acid were situated in the 0.021-17.604 μm range, confirming that this technique measures the agglomerates and not individual particles. TEM measurements confirm the agglomerates formation at low temperatures. For this reason, the analyses of grain size distribution for samples thermally treated at higher temperatures were not realized.

CONCLUSIONS

Nanoforsterite was successfully synthesized by solid state reaction from basic magnesium carbonate and silicon dioxide with and without boric acid and a small excess of silicon dioxide. The XRD patterns showed that forsterite represents the main crystalline phase in samples thermally treated at 1350 °C. The forsterite crystals are well crystallized and the sizes are in the nanometer range. At this temperature, only enstatite as crystalline phases is detected. Small amounts of periclase and enstatite at 1200 °C and 1300 °C temperatures are identified. The mainly crystalline phase in samples fired at low temperatures (800 °C, 900 °C and 1000 °C) is periclase. The crystallites sizes calculated by Scherrer formula for samples fired at high temperatures fall in the nanometer interval. The particles sizes of the treated samples measured by particle size analyzer were situated both in nano and micrometer interval due to the presence of the agglomerates. TEM measurements evidenced the morphology and sizes of forsterite crystals and agglomeration of particles; the size of the individual particles is in the nanometer range.

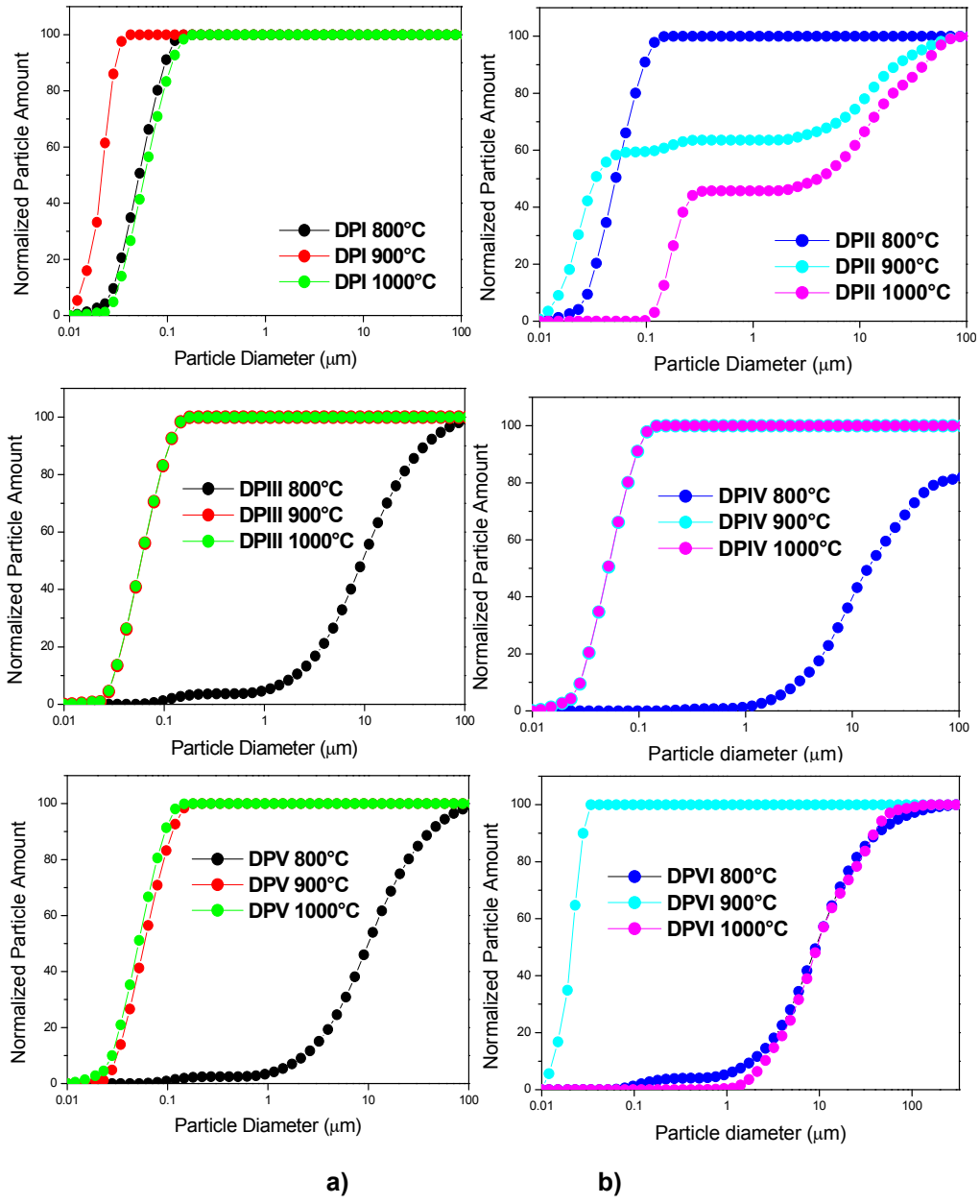

Figure 5. Grain size distributions (cumulative curves) for the forsterite nanopowders synthesized at 800 °C, 900 °C and 1000 °C, (a) samples DPI, DPIII and (b) DPV and DPII, DPIV and DPVI, respectively

EXPERIMENTAL SECTION

Samples preparation

Forsterite (Mg_2SiO_4) powders were synthesized by solid state reaction from basic magnesium carbonate and silicon dioxide. The MgO/SiO_2 molar ratio was established at 2:1, 2:1.05 and 2:1.1. In order to realize a complete reaction between compounds, avoiding the MgO (periclase) presence, and to study the influence of silicium on forsterite biocompatibility a small excess of SiO_2 was added. Boric acid in small quantity was used as a mineralizer. The six mixtures were designed and prepared in laboratory. DPI, DPIII and DPV samples were prepared in a molar ratio of MgO : SiO_2 2:1.05, whereas in DPII, DPIV and DPVI samples the molar ratio was 2:1.10. H_3BO_3 was added, 0.4%wt in DPIII and DPIV, and 0.8%wt in DPV and DPVI, respectively.

A dry homogenization and mechanical activation 4 hours in a Pulverisette laboratory ball mill at ratio material/balls of 1/1.3 was performed. The mean grain size of raw mixtures is ranged between 50-60 nm. The raw mixtures were thermally treated at 800°C, 900 °C, 1000 °C, 1200 °C, 1300 °C and 1350 °C with a heating rate of 2 °C/min and one hour plateau at maximum temperature.

The schematic flow chart for obtaining forsterite nanometer powder is presented in figure 6.

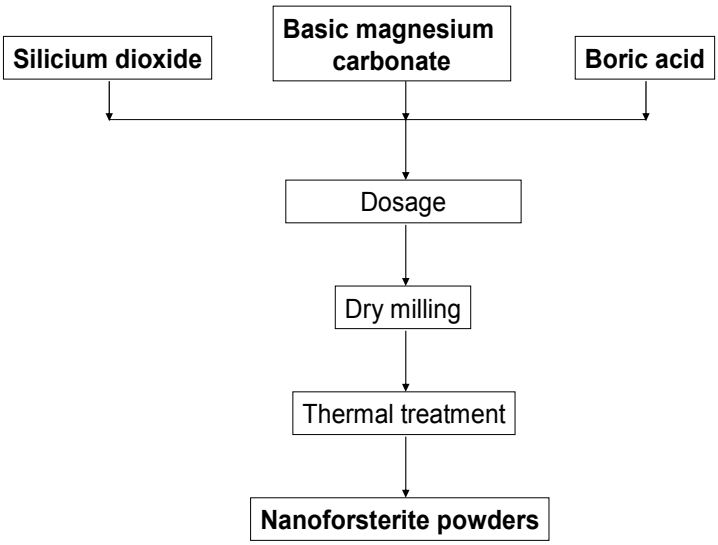

Figure 6. Schematic flow chart of the nanoforsterite synthesis

CHARACTERIZATION METHODS

The prepared materials were characterized by specific oxide materials methods.

X-ray diffraction (XRD)

XRD measurements were performed by a Shimadzu XRD-6000 diffractometer, using CuKα radiation (λ=1.5418 Å), with Ni-filter with a speed of 2°/ min. Scans were conducted from 10 to 90º.

Crystallite size was calculated from XRD data using the Scherrer approximation (Cullity, 1978), according to equation (1):

$$D = K\lambda / h_{1/2} \cos\theta \quad (1)$$

where d is the crystallite size, as calculated for the (hkl) reflections, λ is the wavelength of CuKα radiation, and k is the broadening constant varying with crystal habit and chosen as 0.9 [21].

Particle size analyses

A Shimadzu Sald-7101 laser granulometer was used for investigating the grain size distribution of raw mixtures and forsterite powders. Using this apparatus, serial measurements based on the same measurement principle are possible for particle changing across the 10 nm to 300 μm measurement range.

Transmission Electron Microscopy (TEM)

The size and shape of forsterite crystallites were investigated by transmission electron microscopy (TEM) on HITHACHI H-7650 equipment.

REFERENCES

1. M. Diba, Q.-M. Goudouri, F. Tapia, A.R. Boccaccini, *Current Opinion in Solid State and Materials Science*, **2014**, *18,* 147.
2. M.A. Naghiu M. Gorea, F. Kristay, M. Tomoaia-Cotisel, *Ceramics – Silikáty*, **2014**, *58(4),* 303.
3. M.A. Naghiu, M. Gorea, E. Mutch, F. Kristaly, M. Tomoaia-Cotisel, *J. Mater. Sci. Technol.,* **2013***, 29,* 628

4. C.Y. Tan, R. Singh, Y.C. Teh and Y.M. Tan, *Int. J. Appl. Ceram. Technol.,* **2015***, 12,* 437-442.
5. S.A. Hassanzadeh-Tabrizi, A. Bigham, M. Rafienia, *Materials Science and Engineering C*, **2016,** *58,* 737.
6. M. Kharaziha, M.H. Fathi, *Ceram. Int.*, **2009,** *35,* 2449.
7. M. Kharaziha, M.H. Fathi, *Journal of the Mechanical Behavior of Biomedical Materials*, **2010,** *3,* 530.
8. K.P. Sanosh, A. Balakrishnan, L. Francis, T.N. Kim, *Journal of Alloys and Compounds*, **2010,** *495,* 113.
9. M.H.E. Martin, M., C. K. Ober, C. R. Hubbard, W. D. Porter, O. B. Cavin, *Journal of the American Ceramic Society*, **1992**, *75,* 1831.
10. O. Yamaguchi, Y. Nakajima, K. Shimizu, *Chem. Lett.*, **1976**, *5,* 401.
11. Y. Chen, J. Yu, J. Gao, *Bull. Chin. Ceram. Soc.*, **2012**, *31,* 622.
12. M. Ando, K. Himura, T. Tsunooka, I. Kagomiya, H. Ohsato, *Jpn. J. Appl. Phys.,* **2007**, *46,* 7112.
13. L. Chen, G. Ye, Q. Wang, B. Blanpain, A.Malfliet, M. Guo, *Ceram. Int.*, **2015,** *41,* 2234.
14. S. Sano, N. Saito, S. Matsuda, N. Ohashi, H. Haneda, Y. Arita, M. Takemoto *J. Am. Ceram. Soc.,* **2006**, 89, 568.
15. A.V. Belyakov, N.T. Andrianov, S. S. Strel'nikova, *Inorg. Mater.,* **2012**, *48,* 176.
16. M. Gorea, M.A. Naghiu, M. Tomoaia-Cotisel, G. Borodi, *Ceramics – Silikáty*, **2013,** *57(2),* 87.
17. G.W. Brindley, R. Hyami, *Philos Mag.*, **1965,** 12, 505.
18. F. Tavangarian, R. Emadi, *Powder Technology,* **2010,** *203,* 180.
19. L. Chen, G. Ye, W. Zhou, J. Dijkmans, B. Sels, A. Malfliet, M. Guo, *Ceramics International*, **2015**, *41,* 12651.
20. F. Tavangarian, R. Emadi, *Materials Research Bulletin*, 2010, 45, 388.
21. H.P. Klug, L.E. Alexander, "X-ray diffraction procedures", Wiley, New York, USA, **1956.**